

Structure and properties of the Ivrea body and of the Alps-Apennines system as revealed by local earthquake tomography

D. SCAFIDI¹, S. SOLARINO² and C.EVA¹

¹ *DipTeRis, Dipartimento per lo Studio del Territorio e delle sue Risorse, Università di Genova, Italy*

² *INGV, Istituto Nazionale di Geofisica e Vulcanologia, CNT, clo DipTeRis, Università di Genova, Italy*

(Received May 5, 2005; accepted December 21, 2005)

ABSTRACT The diverse studies carried out with geophysical and geodetic data in the last decades greatly improved the knowledge of the Alps-Apennines system. However, most of these studies were limited to portions of the system or to the shallow structures, and for these reasons reconstruction of the tectonic setting for a larger area and for the deeper layers is still open to different approaches and interpretations; in particular, very little is known about the deeper conjunction between the two chains. In the recent past, many studies have made use of tomographic techniques to investigate the area under study. This paper is the natural extension and completion of the previously published works. Its aim is to propose a more detailed Vp and newer Vp/Vs tomographic images of the Alps-Apennines system and of the Ivrea body by profiting from the increased availability of good S phase pickings and by making use of improved inversion techniques. Some of the main tools developed in the tomographic techniques to evaluate the reliability of the obtained tomo images are used to outline the actual resolution power of the method-data coupling. The inversion results suggest that the Ivrea body may be characterized by a significant anomaly in the Vp/Vs ratio. The conjunction between Alps and Apennines remains partly unresolved due to the complexity of the interacting plates at greater depth.

1. Interaction between three plates: the role of seismic tomography in defining the Alps-Apennines system

For a couple of decades now, the area encompassing the western Alpine Arc, the Ligurian Sea and the northern Apennines (Fig. 1) has attracted the attention of many researchers. In fact, it has been investigated by several geological, geophysical and geodetic techniques (Klingelé *et al.*, 1992; Waldhauser *et al.*, 1998; Schmid and Kissling, 2000; Lippitsch *et al.*, 2003) in an attempt to reconstruct the main tectonic features.

The most recent history of the area started with the continental collision following the closure of the Alpine ocean in the middle Tertiary (around 50 Ma) with a N-S to NNE-SSW directed motion between the European and African plates. The frontal part of the African plate separated, forming the Adriatic microplate and performed an anticlockwise rotation. At deeper levels, a south-dipping continental subduction zone emplaced the European lower crust beneath the African plate, as the interpretation of the EGT seismic data (Blundell *et al.*, 1992) clearly

confirmed. The nearly 1000-km long Alpine orogen, associated with the collision zone, extends from the Ligurian Sea to eastern Austria. Adjacent to the southern rim of the Alps, the northern Apennines mark the collision-generated structure SW of the Adriatic promontory (Giese *et al.*, 1992). They form a WNW to ESE striking orogen that borders the western Alps at its western end and merges to the east with the more NW-SE striking central Apennines. The link between the Alps and the Apennines, Liguria [the Ligurian knot: Laubscher *et al.*, (1992)] in the Genoa region, is extremely complex and still very incompletely exposed.

Seismic tomography is the only technique able to give a comprehensive 3D image of the shallow to asthenospheric structures with the details normally provided by other techniques for much smaller areas. The relatively large wavelengths (up to 10 km) of the earthquakes involved in teleseismic tomography (i.e. the technique making use of very distant epicenters) and the narrow angle of incidence of the teleseismic rays make it useful to describe large structures (Solarino *et al.*, 1996; Di Stefano *et al.*, 1999) while it fails in describing features of low order size and its main limitation is the poor vertical resolution of near-surface structures. As a consequence, this kind of tomography is not appropriate for studies where the goal is a detailed image of shallow and smaller structures, such as this one. The purpose of recognizing the lateral variations of the velocity structure in the crust is, instead, best achieved by local earthquake tomography, that involves earthquakes with higher frequency content occurring at different depths within the study area and thus characterized by a greater variety of the angle of incidence; in particular, this variation is proportional to the location of seismic stations on the surface. It is a straightforward matter that the resolution power of local tomography depends on the areal distribution of seismic recording stations and on the distribution of hypocenters. Unfortunately, both requirements are only partly fulfilled in the area under study (Fig. 1). In fact, five networks [RSNI (Genova, Italy), SED (Zurich, Switzerland), EOPG (Strasbourg, France), Sismalp (Grenoble, France), INGV (Rome, Italy)] own and run stations in the greater Alpine area from the beginning of the 70' and their recordings have been complemented by several temporary installations during field experiments. However, the practicability of installing seismic stations and, as a consequence, their geographical distribution (Fig. 1) is very much influenced by ambient noise and it is biased by geological settings that may decrease the S/N ratio. Consequently, some areas where the sedimentary coverages are relevant (like in the Po Plain) or where the ambient noise is not negligible (like on the coastal zones) do not host seismic stations, leaving parts of the territory not covered by seismic monitoring.

Nevertheless, in the work by Solarino *et al.*, (1997), several thousands of events in the greater Alpine area have been merged, cleaned and relocated according to a common reference velocity model computed for the area. The P readings of 2150 selected events were then used for a tomographic inversion, from which the potential and the limitations of both the data and method applied in that study were revealed.

In the endeavour to enhance the former results, which is the target of the present study, the first step is certainly the addition of new data. The best improvement in the data set comes from enlarging the time span to include the more recently installed seismic stations, that sometimes lie in strategic positions and in most cases are equipped with more performing instruments (three component, broadband or enlarged band sensors); another great improvement comes from considering more and more reliable S phase pickings. The actions taken to get an improved data set are described further on in this paper.

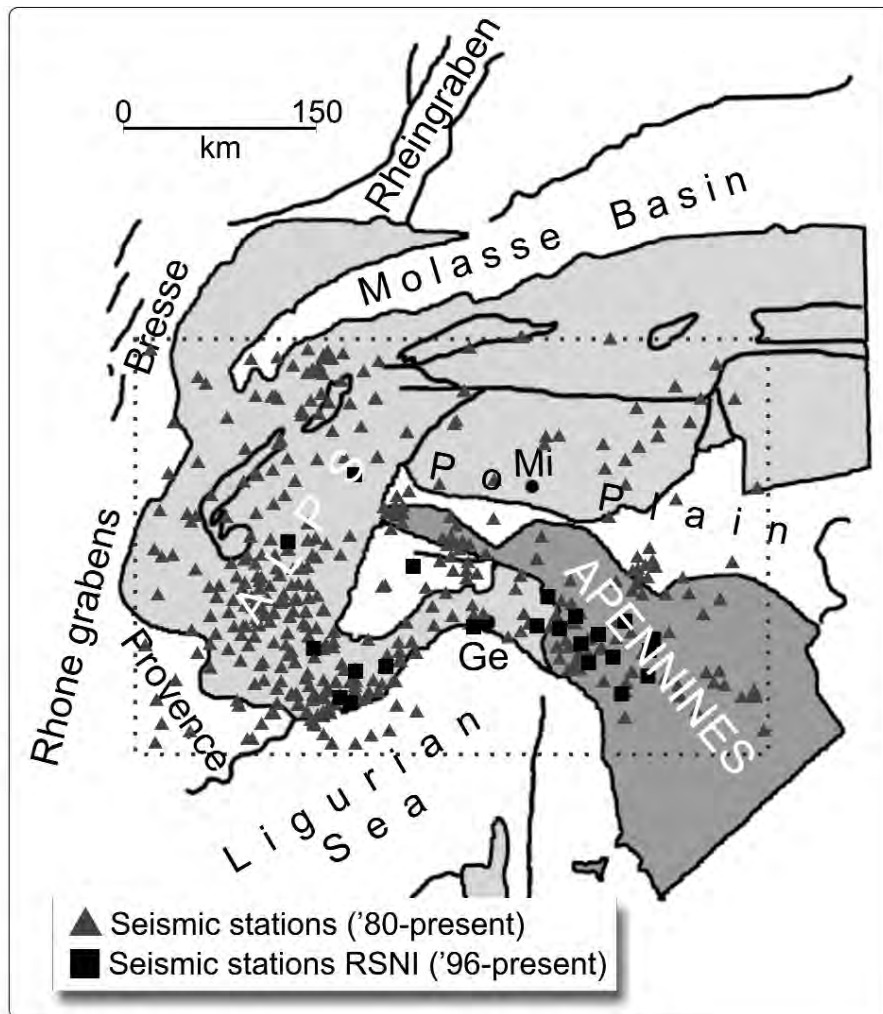


Fig. 1 - General sketch of the Alps-Apennines system. The frame with dots shows the area where tomography has been performed. Triangles mark the locations of the seismic stations (permanent or temporary) installed before 1995; some are longer operating. The squares show the position of those installed after 1996; most are equipped with three-component sensors.

An additional improvement comes from the adoption of updated methodologies. So we propose adopting a more appropriate direct problem in the seismic tomography process [RKP ray-tracing: Virieux and Farra, (1991)]. Overall, the improved approach is potentially able to infer the comprehensive relationship between Alpine and Apenninic chains while being capable of pointing out features sized smaller, to be expected in a very complex structure like the one under study. Nevertheless, the results of a tomographic run are never reliable in the same way on the whole inverted area: while the exact extension of the final resolution can be inferred through resolution estimate tools, a rough a priori estimate can be obtained by running synthetic tests. Both evaluations contribute to avoiding mistaken or uncertain interpretations.

All these details will be clarified in the following paragraphs, after a short discussion on the data used. The last paragraph will deal with the interpretation and discussion of the resulting tomographic images.

2. Data

As previously stated, we based our data set on the selected archive compiled by Solarino *et al.* (1997). The original catalogue of seismicity (2150 seismic events) has been supplemented with arrival times of digital waveform registrations of the RSNI (Regional Seismic Network of northwestern Italy) beginning from year 1996 and relative to events whose location has identical quality properties (20 or more P+S readings, gap < 180°, rms < 1.0 s). The seismic stations of the RSNI network guarantee the coverage of the western Alpine region and, with the most recently installed instruments (black squares in Fig. 1), it also allows the monitoring of the western part of the Po Plain and of the northern Apennines (Solarino *et al.*, 2002). Moreover, the most recent recording stations are equipped with 3-component sensors and wide dynamic digital acquisition systems, which contribute to raising the mean level of quality of the entire data set, and especially the accuracy of the S readings. With this addition, the data set of selected events for the period 1980-2004 rises up to 13,650 earthquakes (in the geographical area extending from 43° 30'N to 46° 30'N in latitude and from 5° 30'E to 12°E in longitude).

It must be pointed out that the distribution of seismicity with depth is not homogeneous in the investigated volume: in fact, the seismicity is prevalent only in the first 25 km of depth (Chiarabba *et al.*, 2005), while there are only a few deeper events. Such a non-homogeneous distribution is not adequate for a tomographic study since it limits the depth of the investigation to the maximum depth of the earthquakes themselves. Moreover, from what stated above, it is clear that the areal distribution of shallower seismic events and of seismic stations is uneven too: this influences the path of seismic rays and results in a strong azimuthal dependence on them.

Two steps were then taken to reduce the effects of these constraints: we decided, a priori, to keep all the 623 events deeper than 25 km in the starting data set and we made a selection of the remaining data using a tool to render “density” of seismic rays as azimuthal-dependent as possible. In fact, all events shallower than 25 km depth have been distributed over a grid of 10 x 10 km assigning only the 5 events with the greater number of P+S phases to each cell. The number of readings varies from 20 to 160. In this way, a consistent reduction is made in areas where seismic events are more numerous, preserving, at the same time, the few earthquakes in lower rate seismicity areas: this ensures ray paths from less sampled directions. Fig. 2, shows the improvement in the distribution of data obtained from the applied selection with regards to a standard quality selection.

The process made 3,521 earthquakes available for the tomographic inversion, for a total amount of 56,833 P phase arrivals times and 41,189 S phase arrival times.

3. Inversion method, parameter settings and reference model

In this work, the iterative simultaneous inversion for 3D velocity structure and hypocenter

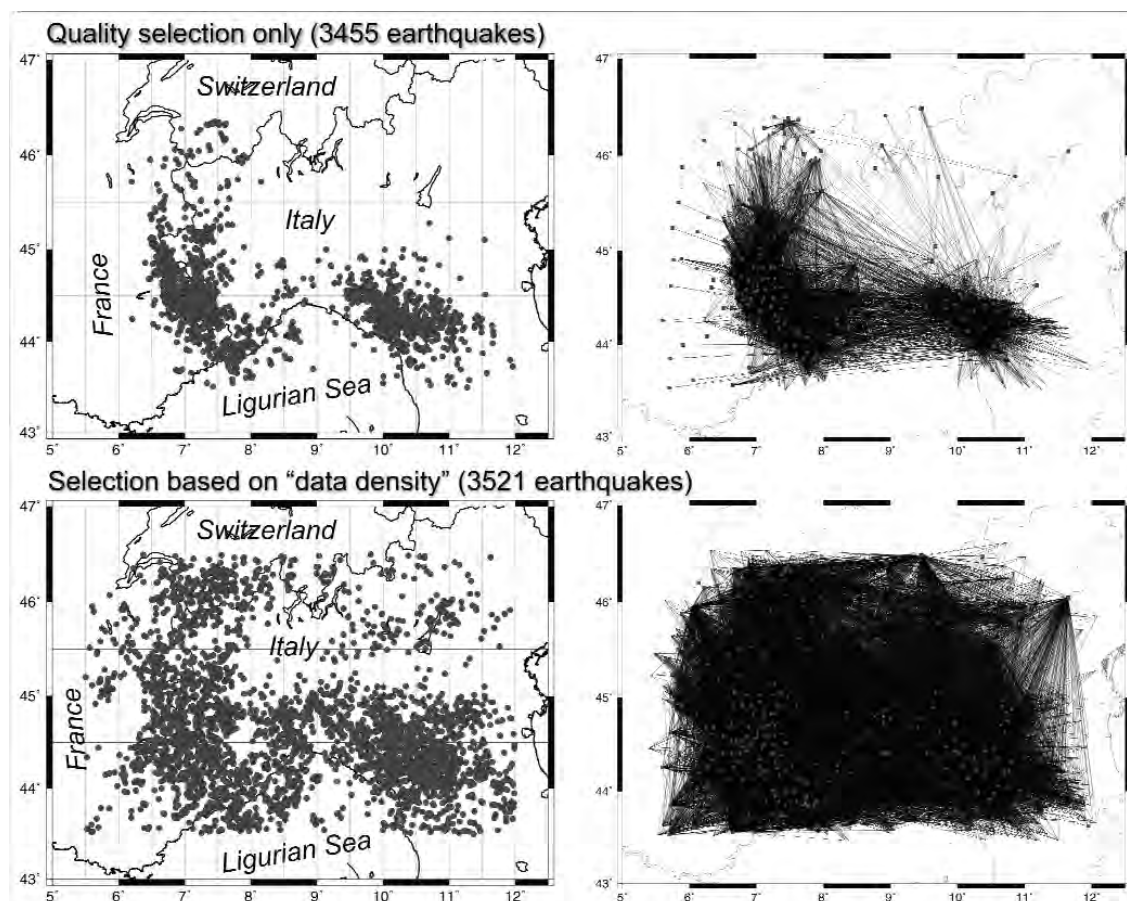


Fig. 2 - Comparison between a standard selection (top panel) and an improved selection to account for “density” of rays. The two selections lead to a similar number of events and comparable overall quality, but the improved routine ensures better and more homogeneous azimuthal coverage (right-hand side).

parameters software Simulps (Thurber, 1983) has been employed. This approach subdivides the problems of the determination of hypocenters and that of the 3D velocity distribution via a parameter separation (Pavlis and Booker, 1980; Spencer and Gubbins, 1980) and then solves the two groups of unknowns separately.

Both problems are non-linear and therefore not directly resolvable, nevertheless they can be linearized and solved iteratively when an initial guess of the velocity model parameters, close enough to the true solution, can be provided. More details and a complete discussion on the theory of inverse problems can be found in Menke (1984). We will come back to the importance of the initial guess in the next few lines.

Once the two problems have been separated, they are solved iteratively in distinct steps: after a first raw location step, adjustments to the initial velocity models (actually V_p and V_p/V_s) are made on the basis of the resulting locations, then the resulting model becomes the current velocity distribution and it is used as an input parameter for the following location step. In this

phase, the inverse problem (solving for 3D velocity) is treated as ill conditioned and therefore solved by a damped least square approach. Basically, it means that the mathematical problem is formulated adding a ε damping value, which must be carefully chosen to render the problem meaningful (Menke, 1984). To avoid any subjective decision, it is very common to plot trade off-curves (Eberhart Phillips, 1989) to determine the best values for the damping.

Once the velocity model has been computed, it is used for the relocation of hypocenters. This part of the problem is solved adopting the Singular Value Decomposition (SVD hereinafter) method. In this case, the quality of the solution depends on the choice of a cut-off value (eigtol hereinafter) that basically sets the number of singular values by shifting the “zero” values to the chosen cut-off value (Menke, 1984).

At the end of the location run, the total data variance is compared with that of the previous step and used for deciding whether to continue iterations or to stop (F-test). The inversion is complete when either an imposed number of iterations is reached or no more iterations, according to the results of the F-test, are possible.

Numerous variables must be provided for the run together with an initial velocity model. Some of these variables can be subjectively chosen and adjusted after the first runs, while for some of them the choice is restricted by the completeness of resolution required by the inversion on one side and by the computational limits on the other side; finally, some others require or simply profit from more rigorous tools for a proper choice.

3.1. Reference model

We already mentioned that the solution of a linearized problem is achievable when the initial guess is very reliable; it is also clear that the quality of any seismic location strongly depends on the velocity propagation model. This basically means that the choice of a correct velocity reference model in tomographic problems is of paramount importance (Kissling *et al.*, 1994) since it deals with both aspects.

Solarino *et al.* (1997) proposed a 1D reference model, based on the 1D inversion of a great number of local earthquakes, of the enlarged Alpine area for both location and tomographic purposes. This model and the relative station corrections do not take into account the stations installed after 1995, and thus needed upgrading. The operation would simply consist in a run with model and locations held fixed, and station delays free to float (Kissling *et al.*, 1995). However, in order to adapt the model for the tomographic run, it is necessary to incorporate the effect of the station delays in the velocity distribution. In fact, they account for a substantial part of the effects of the local near-surface velocities that are also target of the tomographic inversion; it is then recommendable not to have a separate picture of 3D anomalies and station delays distribution, which are interdependent. The initial reference model is then designed, in this case, not to account for the station corrections. The improved model is shown in the left panel of Fig. 3. The S-velocity model has been obtained by applying a V_p/V_s ratio derived from the Wadati diagram (Evans *et al.*, 1994).

Eventually, the starting model will have to be properly parameterized to be used as input by Simulps, which requires a velocity distribution for specified depths and a gradient between these “surfaces”. Therefore the 1D model, originally organized in layers of constant velocity, has been adapted before its usage in the tomo process.

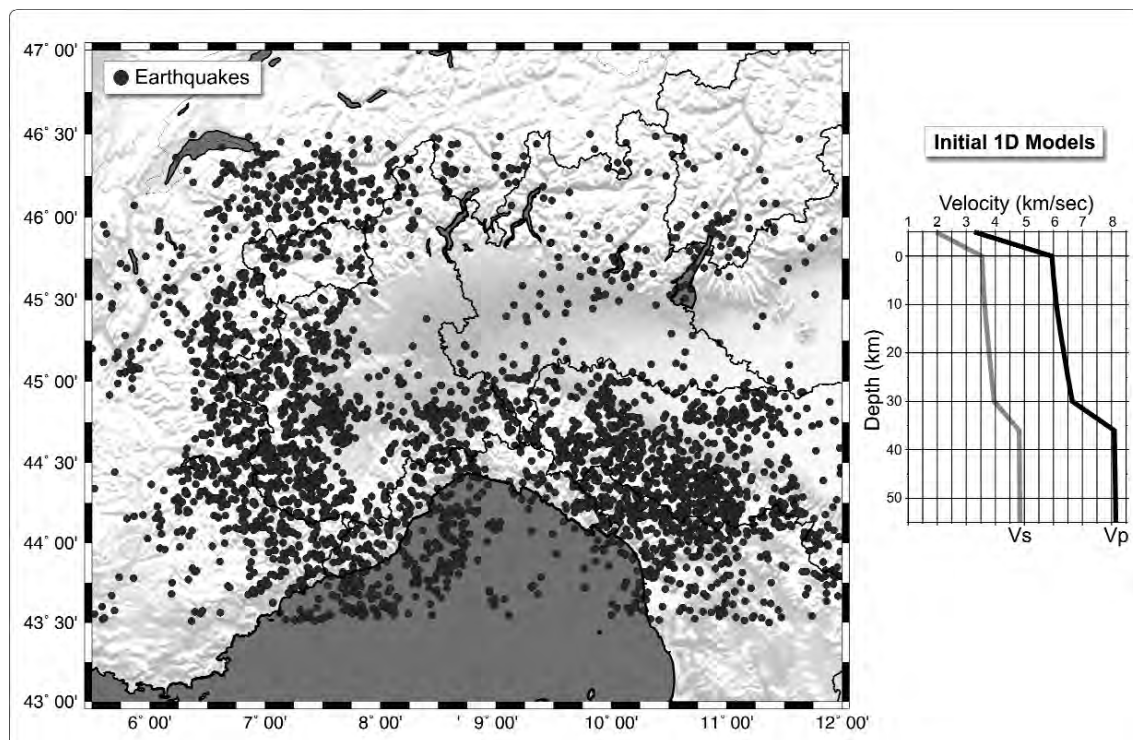


Fig. 3 - Left: spatial distribution of the earthquakes used for the tomographic inversion. Right: initial 1D P and S models (Solarino *et al.*, 1997).

3.2. Damping values and SVD cut-off parameters

As stated above the choice of some parameters cannot be made on a subjective basis. This is the case of the variables that rule the mathematical routines for data inversion.

Eberhart Phillips (1989) has suggested selecting the damping (the damping factor in the damped least square problem) by plotting curves of trade-off between data variance and solution variance from single iteration inversions: the optimal value of damping is the one that allows a great (possibly the greatest) reduction in the data variance with a moderate increase in the solution variance. Since the improvement of data variance results from the coupled inverse problem (adjustment to the velocity model + relocation of events with the varied model), and the way the model changes on each run depends on the locations, we propose to plot enhanced trade-off curves that take into account a variety of SVD eigtol values for each damping applicable to the velocity inversion part.

Fig. 4 shows an improved version of the trade-off curves where both parameters (SVD cut-off values and damping) are taken into account. Numerous such plots have been drawn to display the dozens of attempts in the search of the best set among several pairs (V_p+V_p/V_s) of damping values and many SVD cut-offs for each pair. It turned out that 0.045 (eigtol), 50 and 80 (V_p and V_p/V_s damping) perform very well. Several tests, including plots of the ratio between maximum and minimum eigenvalues for each event, confirmed the correctness of the choice.

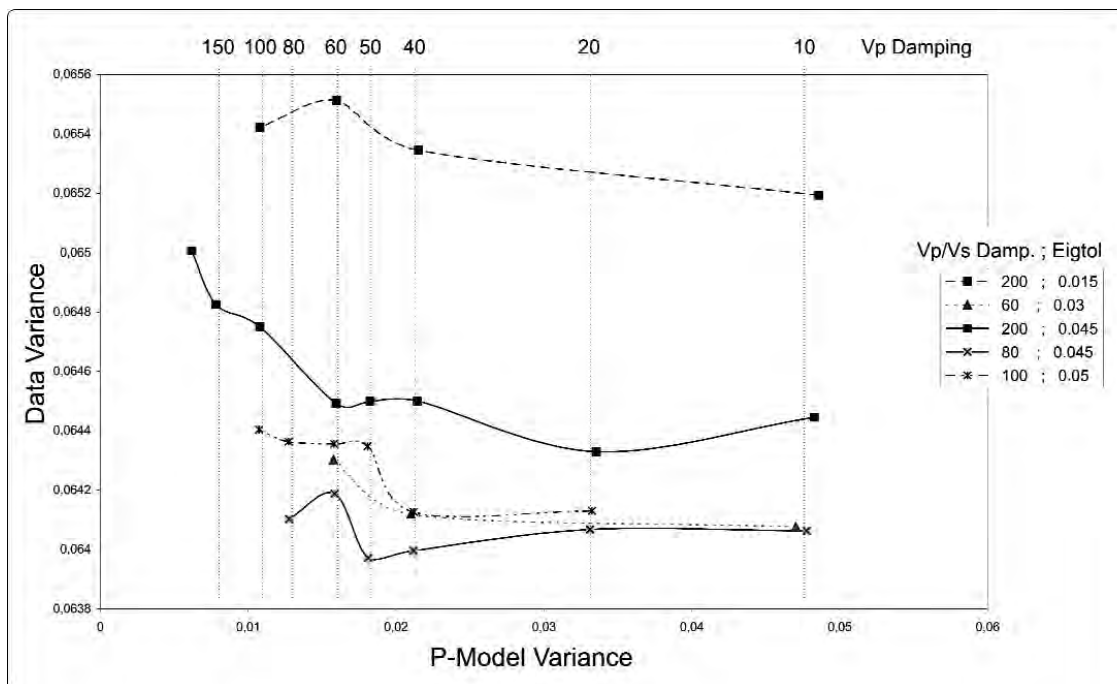


Fig. 4 - Improved trade-off curves for selecting correct Vp, Vp/Vs damping and cut-off for SVD location problem. Each point of the graph represents a triplet of values and the effect of each triplet can be extracted from the joint reading of the corresponding X-axis value (variance of the velocity propagation model for P waves) and Y-axis value (variance of the data). The triplet 50, 80, 0.045 ensures a significant decrease of data variance without affecting the P-model variance. Similar curves are produced for the Vp/Vs model.

4. Reliability of tomographic results

The reliability of any tomographic result may vary significantly within the inverted area and must be estimated before any interpretation is made. There are several “a posteriori” tools that either provide an estimate of the mathematical resolution (like the analysis of the resolution and covariance matrices) or show the illumination properties of the data set [the weighted ray lengths (Thurber, 1983; Eberhart Philips, 1989) or the ray density tensors (Kissling, 1988)]. In principal, however, these resolution estimates only yield information about the quality of the solution assuming appropriate model parametrization. They offer no means of assessing the validity of this parametrization.

The best, presently available tools, to study the effects of a particular model parametrization or of a particular choice of forward or inverse solution are synthetic data tests using a synthetic 3-D velocity model that mimics expected or a priori-known real structures.

According to Kissling *et al.* (2001), these tests are needed to guide the choice of the parametrization of the problem and, only upon such calibration, combined resolution estimates [(Resolution Diagonal Elements (RDE), Spread function (SPR), ray density tensors, partial

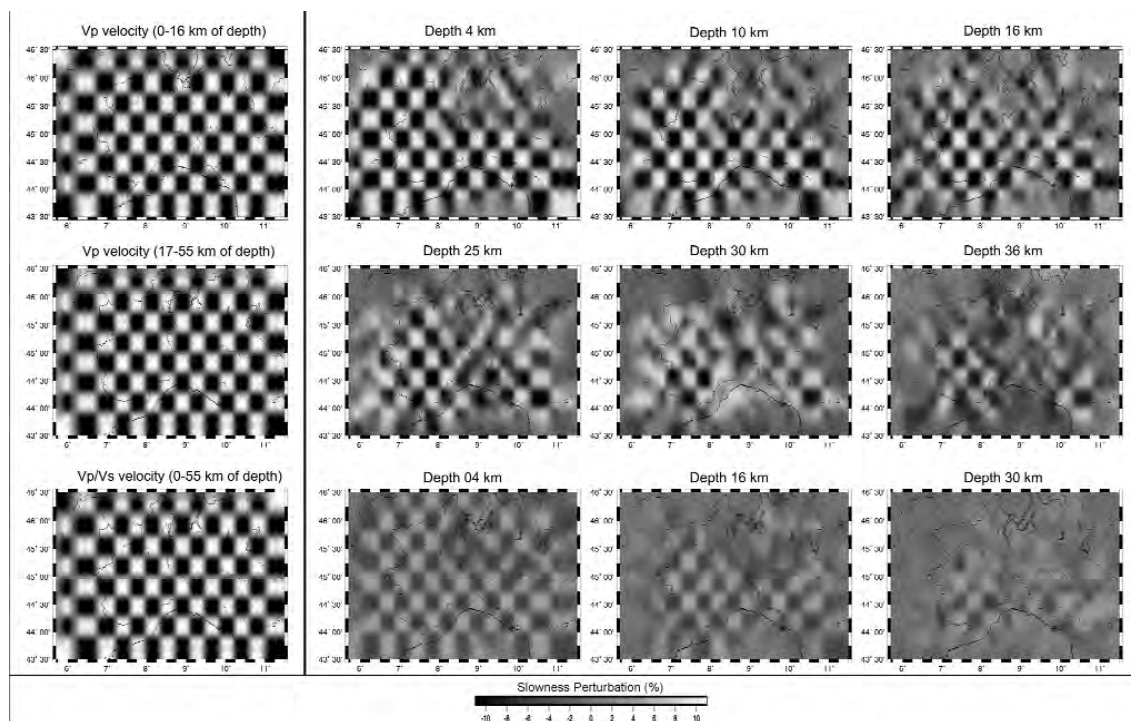


Fig. 5 - Checkerboard tests. Left: synthetic models; right: restored anomalies. The upper two lines show tests for V_p , the bottom for V_p/V_s .

derivative weight sums (DWS), total number of hits per cell (HIT)] provide excellent and detailed information about the laterally variable resolving power of the data set for any particular application.

The synthetic tests are, in a way, a priori tools and will be treated first. All synthetic data have been obtained by applying a special feature of the Simulps code; the computation consists in adding the contribution of the ray path to the observed travel time through the anomalies of the synthetic model as resulting from a three-dimensional ray tracing; the location parameters are not changed.

The information that can be derived from the classical checkerboard resolution tests is limited, so to give it more significance, we performed not only a regular test but also a velocity inversion (alternation of negative and positive values for overlaid layers) at a 16-km depth. We show the results of the reconstruction for both V_p and V_p/V_s only for this more complicated model. Fig. 5 shows some of the layers (4, 10, 16, 25, 30, 36 km depth for V_p and 4, 16, 30 km for V_p/V_s), from which it can be inferred that the 3-D velocity model can be reconstructed down to a 36 km and a 30-km depth, respectively, for V_p and V_p/V_s , with greater accuracy in the central part of the area.

The checkerboard test has the only purpose of grossly defining the areas where an acceptable reconstruction of predefined structures is achievable. To better discover how much the tomographic inversion is able to recreate the real geometries of the crustal and subcrustal

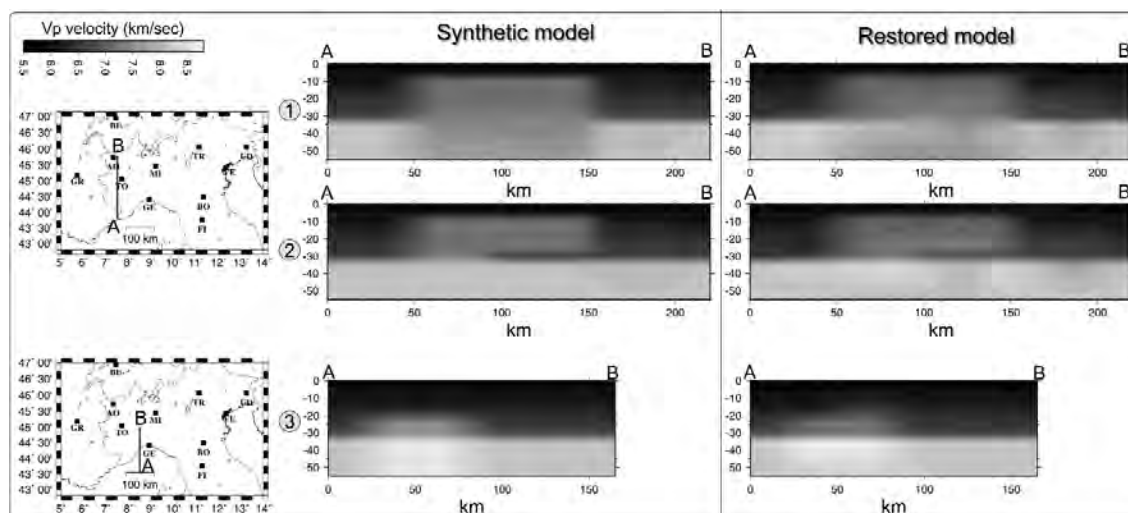


Fig. 6 - Synthetic models (center) and restored anomalies (right). In profile 1, the anomaly is a 45 km thick body with different velocities in its upper and lower parts. In profile 2, the shape of the anomaly resembles a flipped L. In profile 3, it is a 35 km thick box of two velocities. The different velocities for the upper and lower parts are necessary for the body to have the same velocity percentage value.

structures, we developed a synthetic 3D model with two high velocity bodies and geometry comparable to what we expect for the “Ivrea” body and for the region of the uplift of the Ligurian Moho. Concerning the possible shape of the first, we made two different models to account for the possibility that the body is unique or fragmented. For convenience, both reference and restored models are plotted in cross-sections. In one test, we used one box extending from north to south, 45 km thick (from a 10 to 55-km depth) having two slightly different velocities (Fig. 6, 1, center); in the other test, the box has a shape resembling a flipped L, such as a body that has a “root” in the deeper layers would be (Fig. 6, 2, center). Finally, (Fig. 6, 3, center) mimics the uplift of the Ligurian Moho.

Analyzing the results of this second series of synthetic tests (Fig. 6, right side), we can infer that the tomographic inversion defines shapes of bodies introduced and it also has the power of clearly distinguishing between a unique body (panel 1) and two different geometries (panel 2), at least in the region where we expect to discover the high velocity “Ivrea” body. This is very important since the shape of the body, and in particular its extension with depth, is still very controversial. A little smearing is observed at the borders of the resulting anomalies, partly due to the graphic plotting routines (it affects also the imposed model) and partly to a non-complete resolution. This smearing is of the order of 0.1-0.2 km/s.

Regarding the a posteriori assessments, one very rough, and sometimes misleading way of assessing the illumination of tomographic results, consists in plotting the hit count, which sums up the rays that contribute to the solution at each node. The information contained in the hit count values is incomplete, because it does not carry any detail about the azimuthal coverage of the rays. In fact, all rays coming from the same azimuth and distance provide similar information (and contribute only once to the “illumination” of the node). However, the careful selection of

data in this work has already partially accounted for azimuthal homogeneity (as discussed in Fig. 2); therefore, we assume that the “density” of rays is close to the best that data can provide.

One of the most powerful tools for assessing mathematical resolution is certainly the resolution matrix, that coincides with an identity one when each model parameter is determined uniquely. Each row of the matrix describes the dependence of one model parameter on all other parameters of the model. A rigorous display of the elements of this matrix is not easy to achieve, since it requires a 3D image per model parameter. Many recent papers describe innovative methodologies to deal with the resolution and error estimates in seismic tomography (De Natale *et al.*, 2004), but in our study, we prefer to approach the topic using more standard methodologies.

In practice, a quick and powerful way of checking the general appearance of the resolution matrix is to take into account its diagonal elements (RDE hereinafter): this does not ensure that all non-diagonal values are zero, but it does provide a quick and qualitative insight into how well the solution has been reached. Unfortunately, the diagonal values, that depend strongly on the damping used, suffer from a certain subjectivity since a lower and an upper limit must be arbitrarily chosen within the possible values. In fact, while it is clear that a value zero means no solution and a value one means a “perfect” resolution, one must decide how to treat the intermediate values, that are the most numerous. The choice cannot be led by any objective criterium, since Haslinger (1998) has shown that not even specific synthetic tests can define threshold values for resolution estimates. The distribution of RDE values suggests fixing 0.1 as the minimum to trust the solution and 0.5 as a reference for fair-to-good resolution. It is worth noting that this choice is somehow arbitrary, but within the area circumscribed by the 0.5 contour, there are sectors where the RDE values may reach 1.0, that means a “perfect” resolution.

5. Tomographic images

Keeping in mind that only the tomographic images that respond to the requirements for reliability deserves interpretation, we have indicated, with contoured lines, the areas that meet such conditions. The results are shown as plain views (images of horizontal slices for each selected depth) and as cross-sections. To avoid any artificial interpretation and possibly the smearing, the velocity V_p or the V_p/V_s ratio scales are continuous.

Fig. 7 shows the plane views relative to V_p percentage velocity change (with respect to the mean velocity of each layer) for a 0, 4, 10, 16, 25, 30, 36-km depth. Colours range from reddish (low P velocities) to bluish (high P velocities). As expected, the reliability of the results strongly decreases deeper than 25 km, and it is low at a 36-km depth. Regarding the readability of the results, the shallow tomographic images have a spot-like appearance and, in the upper layer in particular (0 km), this is so remarkable that the observer recognize the inversion nodes; below a 4-km depth this fuzzy characteristics disappears, and anomalies are less sparse.

The main features that can be derived from the analysis of these images are: the presence of a high-velocity body (with its northern limit in correspondence to the Ivrea area) that seems made of two distinct pieces at a depth shallower than 16 km and becomes united lower down; the existence of a high-velocity area in the Ligurian Sea from 16 km depth and deeper; a low-velocity area, almost corresponding to the Po Plain, which is as thick as 16 km.

Plane views give a good comprehensive frame of the distribution of anomalies but are very

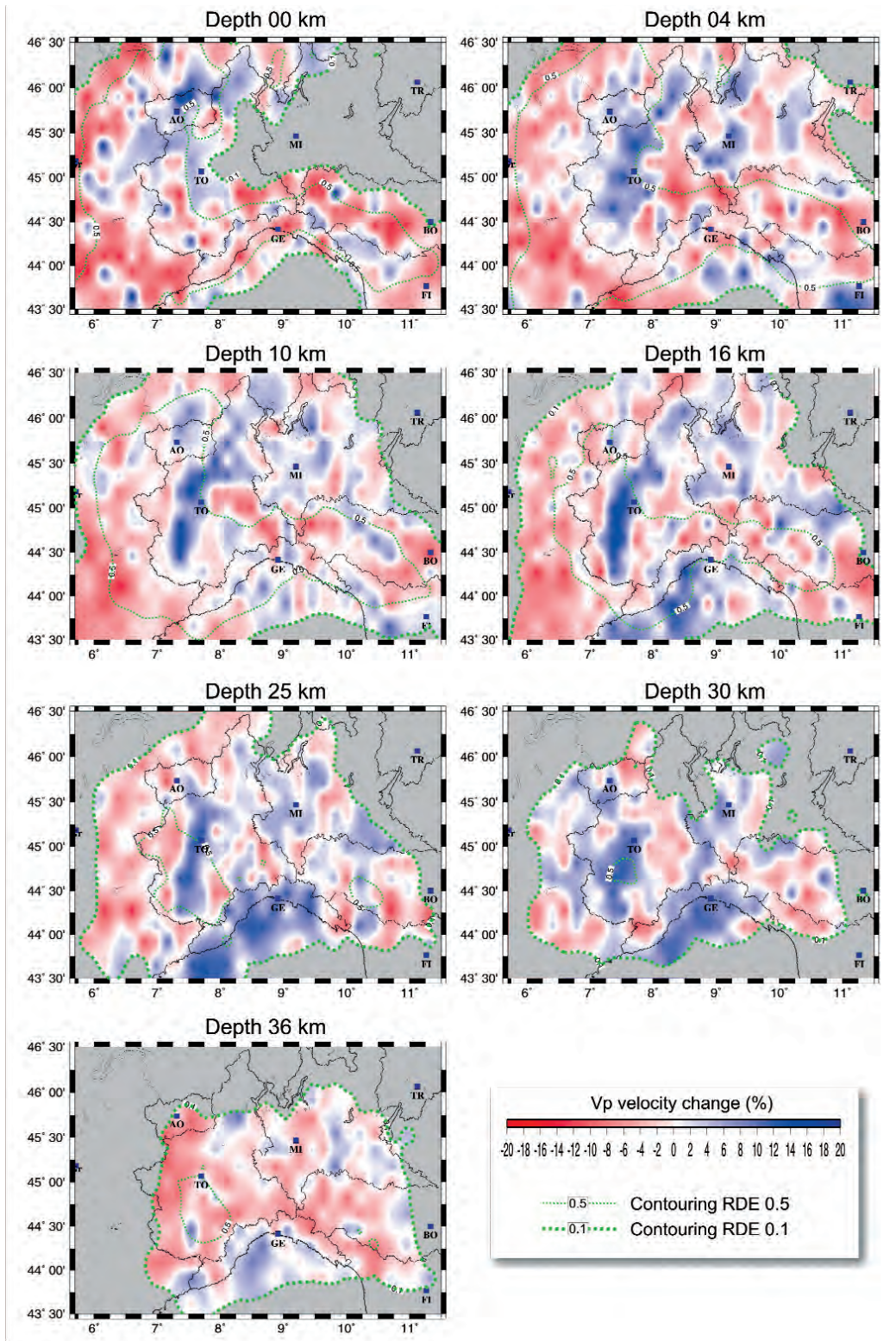


Fig. 7 - Results of tomography in plane view. The layers at 0, 4, 10, 16, 25, 30, 36 km are reported in velocity percentage change with respect to the average for each layer.

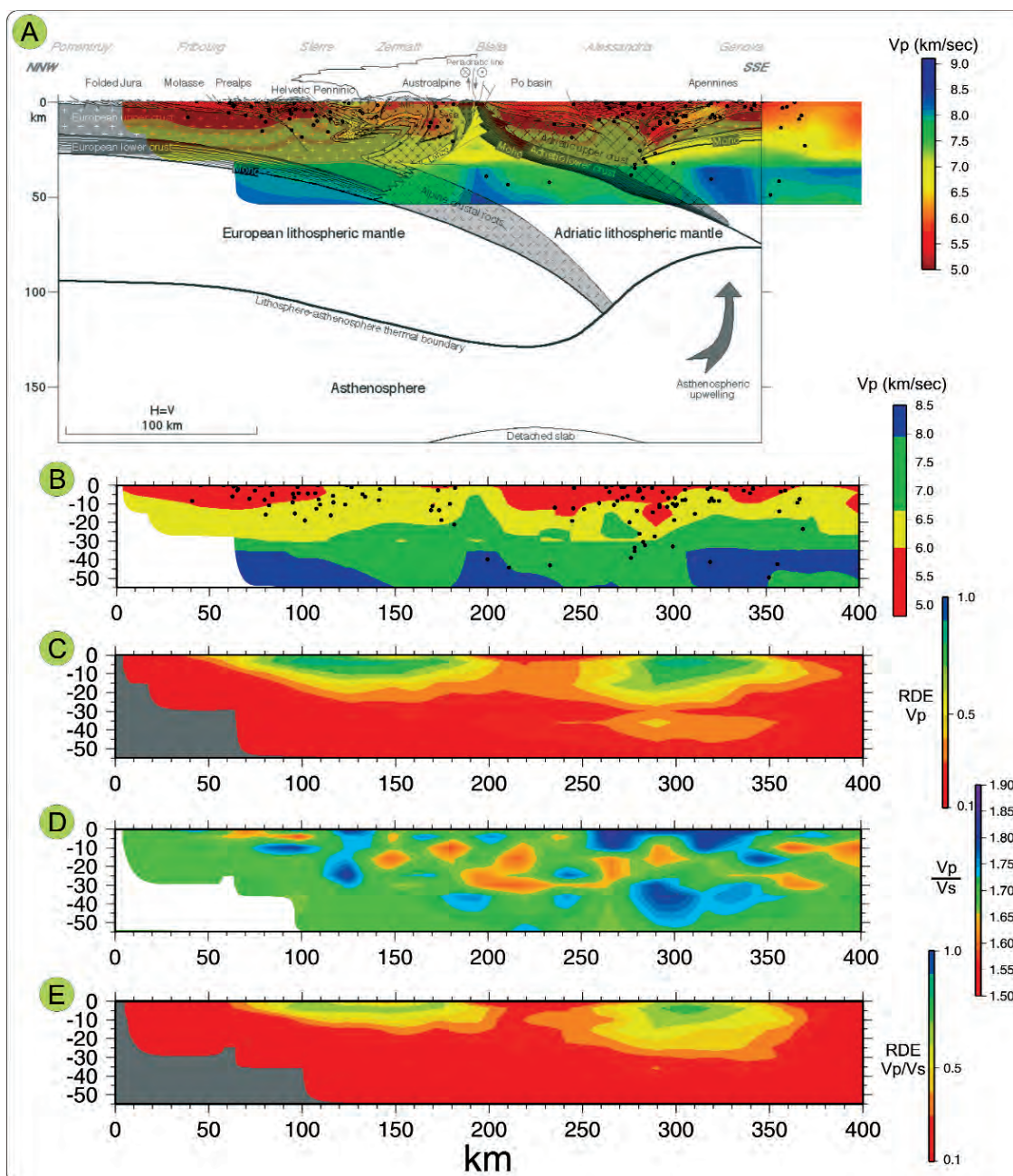


Fig. 8 - Tomographic cross-section along a modified NFP 20 profile (A); tomographic cross-section for discrete velocities (B); Resolution diagonal elements along the cross-section (C); Vp/Vs ratio (D). Gray colour marks area where the RDE values are less than 0.1, the lower threshold for solution reliability (see text).

difficult to interpret. For this reason, we present a couple of tomographic cross-sections for both Vp and Vp/Vs. For convenience, they are superimposed on interpreted cross-sections resulting from other studies, in a sort of validation process. In particular, since we are interested in having

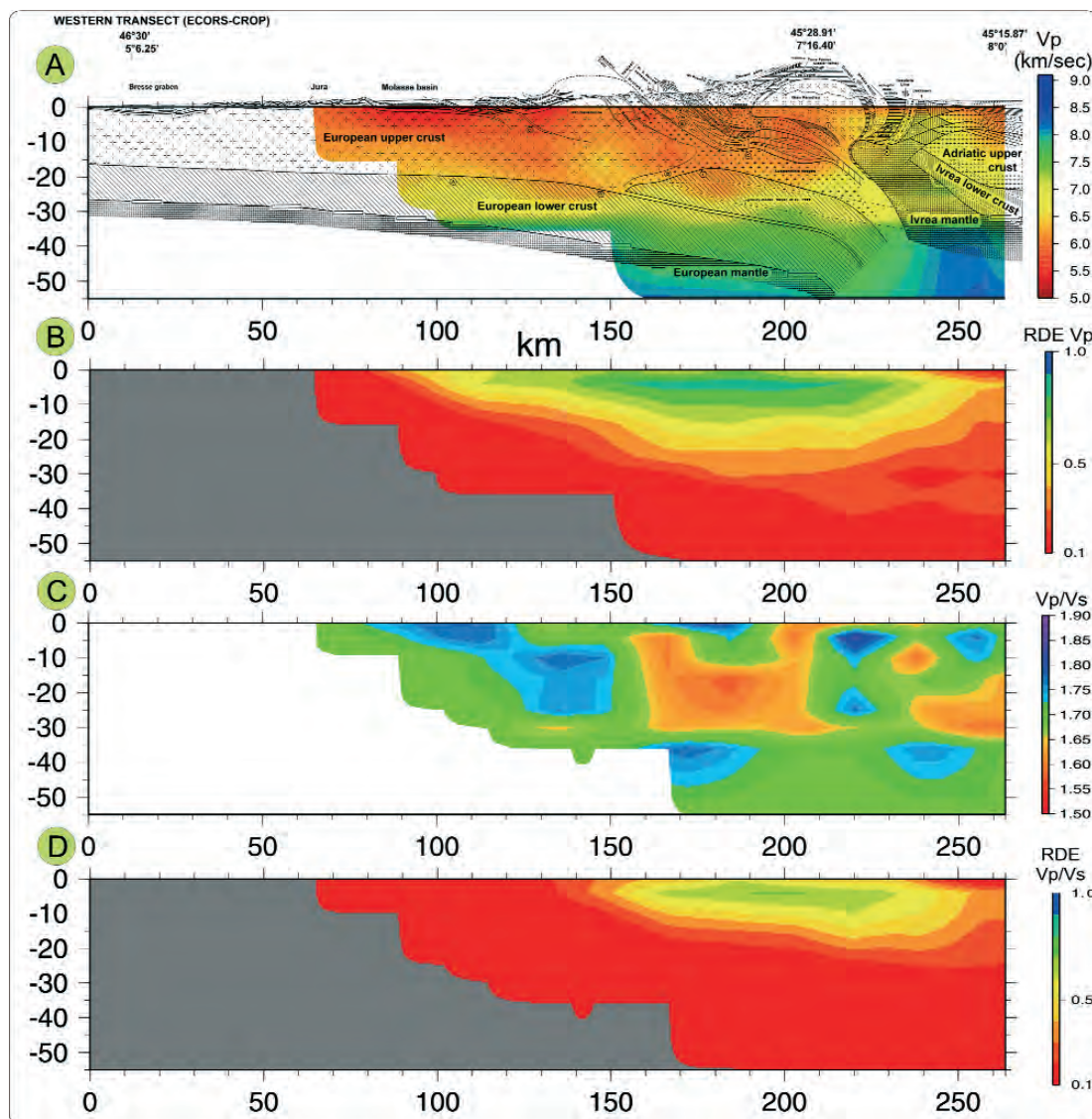


Fig. 9 - Tomographic cross-section superimposed on the ECORS-CROP line (A); Resolution diagonal elements (B); Vp/Vs ratio (C). Gray colour marks the area where the RDE values are less than 0.1, the lower threshold for solution reliability .

more details on the geophysical Ivrea body and on the relationships between Alps and Apennines, the results of the ECORS-CROP and NFP 20 experiments are used for reference. A detailed description of these two fundamental experiments can be found in Roure *et al.*, (1990) and Pfiffner *et al.*, (1997), respectively.

Fig. 8 A shows tomographic results superimposed on an extra-processed NFP 20 cross section (http://www-sst.unil.ch/research/seismic/W_Alps.htm). The main differences with the original

plot are the extension to the south of the line (that here reaches the Ligurian Sea south of Genova), the addition of the possible deep and lithospheric structures as obtained by teleseismic tomography (Spakman *et al.*, 1993) and the addition of the results from the gravity modelling along the NFP 20 line.

The comparison between our results and the NFP 20 cross-section are extraordinarily encouraging, especially if one keeps in mind that some differences may depend on a slightly different orientation of the sections and on the fact that the NFP 20 section is already an interpretation rather than a raw data plot.

In particular, the subduction of the European lower crust under the Adriatic crust is clearly evident; we propose a more vertical character for the geometry of this subduction, with a sharper bend towards the mantle. In Fig. 8, the upwelling of the Ligurian Moho under Genova (right hand side of the figure) is also very clearly visible.

Moreover, the distribution of P seismic velocity well reflects the sediments of the Po Plain (red areas, low velocity) and the Mount Rosa massif. Regarding the Ivrea body, it clearly belongs to the Adriatic sector: it appears as a body included in the crustal doubling, detached from the Adriatic Moho and having mantle characteristics lower than a 30-km depth, while it has velocity of lower crust at shallow depth. Its outcrop has similar characteristics: we then propose that no mantle material outcrops in the Ivrea area. The roots of the Ivrea body are directly connected to what Spakman *et al.* (1993) call the Adriatic lithospheric mantle, and the apparent connection with the European Moho (Fig. 8, panel A) is only due to the proposed geometry of the latter, sensibly less bent than what our tomographic images suggest.

In an attempt to simplify the interpretation, different colour sequences, based on existing Earth models, have been used to draw the plots. In cartoon B of Fig. 8, colours are grouped according to those proposed by PREM (Dziewonski and Anderson, 1981), but slightly adapted. Red is used for sedimentary materials, yellow for the upper crust, green for the lower crust and blue for the upper mantle material. All features described for panel A become more evident, especially for what concerns the Ivrea body. Its shallow part appears as if made of lower crust material rather than of mantle rocks, as if it were made of two distinct pieces. Panel C, shows the reliability of both images: the Ivrea area is characterized by a lower range of RDE values, therefore minor adjustments in the velocity may derive from increasing the resolution in that sector. Reaching velocities larger than 7.5-7.6 km/s does not, in any case, seem likely.

Another important feature of the Ivrea area can be inferred from the distribution of the V_p/V_s ratio (panel D in Fig. 8). It clearly appears that the Ivrea body is characterized by a low V_p/V_s ratio anomaly, unlike that expected for a deep body. This anomaly almost coincides with the shallow part, the one characterized by lower velocities.

Fig. 9 shows the comparison between the ECORS-CROP findings and the tomographic cross-section drawn along a similar orientation. Even in this case, it is clearly evident that the Ivrea body does not exceed, 7.1-7.2 km/s in its shallow part.

6. Discussion and conclusions

The use of an improved tomographic inversion program performed on numerous P and S phases has inferred some more details on the relationship between the Alps and the Apennines

and has given additional constraints to the characteristics of the Ivrea body. In particular, the main improvement follows from the capacity of the adopted ray tracer to take into account longer rays and, as a consequence, to increase the cross-firing and the deep sampling.

Several issues can be derived from the observation and interpretation of the obtained results. The main features of the Alps-Apennines system, as obtained from other studies, are all confirmed but sometimes slightly rearranged, in particular, with respect to their geometry and extension. For example, the bend in the subduction of the European Moho is supposed to be sharper than the results of the NFP 20 line proposed.

One of the most important findings is that the Ivrea body appears, in our tomographic reconstruction, as a body with a different value of V_p/V_s with respect to the surrounding rocks. We propose that the so-called geophysical Ivrea body has no material with mantle velocity in its shallow part, conversely to proposals, for example, by Schmid and Kissling, (2000). They based part of their study on the tomographic studies of Solarino *et al.* (1997) and suggested that an increase of 6 to 8% in the reference velocity could justify velocities typical of a mantle. We rather believe that the shallow part of the Ivrea body was originally made of mantle material that, after being subjected to strong modification due to complex processes during its emplacement, lost part of its transmittal characteristics. In such a case, however, we should observe a high V_p/V_s ratio, which is not found. Another possible interpretation is that Ivrea is made of lower crust material only and preserves its low V_p/V_s ratio, typical of a deep material. In fact, it is well known that V_p/V_s ratio tends to decrease with depth, due to fluid loss and consequent increase of the V_s velocity. Finding such a ratio at shallow depth might be index of ascended material.

Regarding the Alps-Apennines system, the conjunction between the two chains is masked by the Po Plain; this structure is clearly delineated in the cross-sections, and its nature is confirmed by the relatively high V_p/V_s ratio, expected for sediments where transmittance of V_s waves is biased by porosity and fluids. The complexity of the Alps-Apennines system is anyway confirmed by the apparent link between the Ligurian and Adriatic Moho.

Finally, it is noteworthy that most of the shallow seismicity of the Po Plain in the NFP 20-like cross-section is actually due to the direction of the line, which cuts the area of Asti (southern Piedmont) where numerous earthquakes occurred in the past years. From the tomographic images, it seems that this seismicity is induced by tectonic events occurring at a much greater depth and transferring stress to shallower layers. The collection of more data, and, possibly, the installation of more seismic stations in the area, will help investigate this aspect.

Acknowledgements. Edi Kissling and Giuseppe de Natale reviewed the paper. Their comments and suggestions greatly improved the manuscript. This study is part of the MIUR 2004 project funded under contract prot. 2004045141_006.

REFERENCES

- Blundell D., Freeman R. and Mueller St.; 1992: *A continent revealed - The European geotraverse*. Cambridge Univ. Press, 275 pp.
- Chiarabba C., Jovane L. and Di Stefano R.; 2005: *A new view of Italian seismicity using 20 years of instrumental recordings*. Tectonophysics, **395**, 251-268.
- De Natale G., Troise C., Trigila R., Dolfi R. and Chiarabba C.; 2004: *Seismicity and 3D sub-structure at Somma-Vesuvius volcano: evidence for magma quenching*. Earth Plan. Science Lett., **221**, 181-196.
- Di Stefano R., Chiarabba C., Lucente F. and Amato A.; 1999: *Crustal and uppermost mantle structure in Italy from the inversion of P-wave arrival times: geodynamic implications*. Geophys. J. Int., **139**, 483-498.
- Dziewonski A.M. and Anderson D.L.; 1981: *Preliminary reference Earth model*. Phys. Earth planet. Inter., **25**, 297-356.
- Eberhart Phillips D. M.; 1989: *Investigation of crustal structure and active tectonic processes in the coast ranges, central California*. PhD thesis, 209 pp.
- Evans J.R., Eberhart Phillips D. and Thurber C.H.; 1994. *User's manual for Simulps12 for imaging V_p and V_p/V_s : a derivative of the "Thurber" tomographic inversion Simul3 for local earthquakes and explosions*. USGS Open file report 94-431, 100 pp.
- Giese P., Roeder D. and Scandone P.; 1992: *The fragmented Adriatic microplate: evolution of the Southern Alps, the Po basin and the northern Apennines*. In: Blundell D., Freeman R. and Mueller St. (eds), *A Continent Revealed - The European Geotraverse*, Cambridge Univ. Press, Cambridge, pp. 190-199.
- Haslinger F.; 1998: *Velocity structure, seismicity and seismotectonics of northwestern Greece between the Gulf of Arta and Zakynthos*. PhD thesis, 160 pp.
- Kissling E.; 1988. *Geotomography with Local Earthquake Data*. Reviews of Geophysics, **26**, 659-698.
- Kissling E., Ellsworth W.L., Eberhart Phillips D.M. and Kradolfer U.; 1994: *Initial reference models in local earthquake tomography*. J. Geophys. Res., **99**, 19635-19646.
- Kissling E., Solarino S. and Cattaneo M.; 1995: *Improved seismic velocity reference model from local earthquake data in Northwestern Italy*. Terra Nova., **7**, 528-534.
- Kissling E., Husen S. and Haslinger F.; 2001. *Model parametrization in seismic tomography: a choice of consequence for the solution quality*. Phys. Earth Planet. Inter., **123**, 89-101.
- Klingel  E., Lahmeyer D. and Freeman R.; 1992: *EGT: gravity anomaly map, Central and Southern segments*. In: Blundell D., Freeman R. and Mueller St. (eds), *A continent revealed, the European Geotraverse*, Cambridge University Press, New York.
- Laubscher H., Biella G.C., Cassinis R., Gelati R., Lozej A., Scarascia S. and Tabacco I.; 1992: *The collisional knot in Liguria*. GeolRund., **81**, 275-289.
- Lippitsch R., Kissling E. and Ansorge J.; 2003: *Upper mantle structure beneath the Alpine orogen from high-resolution teleseismic tomography*. Jour. Geoph. Res., **108**, 2376-2391.
- Menke W.; 1984: *Geophysical data analysis: discrete inverse theory*. International Geophysics Series, 45, Academic Press, 289 pp.
- Pavlis G.L. and Booker J.R.; 1980: *The mixed discrete-continuous inverse problem: application to the simultaneous determination of earthquake hypocenters and velocity structure*. J. Geophys. Res., **85**, 4801-4810.
- Pfiffner O.A., Lehner P., Heitzman P.Z., Mueller S. and Steck A.; 1997: *Deep structure of the Swiss Alps - Results from NRP 20*. Birkhauser AG., Basel, 380 pp.
- Roure F., Heitzmann P. and Polino R.; 1990: *Deep structure of the Alps*. M m. Soc. g ol. Fr. 156; M m. Soc. G ol. Suisse 1; Soc. Geol. Ital., 367 pp.
- Schmid S.M. and Kissling E.; 2000: *The arc of the western Alps in the light of the geophysical data on deep crustal structure*. Tectonics, **19**, 62-85.
- Solarino S., Ferretti G. and Eva C.; 2002: *Seismicity of Garfagnana-Lunigiana (Tuscany, Italy) as recorded by a network of semi-broad-band instruments*. J. of Seism., **6**, 141-152.
- Solarino S., Spallarossa D., Parolai S., Cattaneo M. and Eva C.; 1996: *Litho-asthenospheric structure of northern Italy as inferred from teleseismic P-wave tomography*, Tectonophysics, **260**, 271-289.
- Solarino S., Kissling E., Sellami S., Smriglio G., Thouvenot F., Granet M., Bonjer K. P. and Slejko D.; 1997:

Compilation of a recent seismicity data base of the greater Alpine region from several seismological networks and preliminary 3D tomographic results. Annali di Geofisica, **40**, 161-172.

Spakman W., van de Lee S and van der Hilst R.; 1993: *Travel time tomography of the European-Mediterranean mantle down to 1400 km.* Phys. Earth. And Planet. Int. **79**, 3-74.

Spencer C. and Gubbins D.; 1980: *Travel time inversion for simultaneous earthquake location and velocity structure determination in laterally varying media.* Geophys. J. Roy. Astr. Soc., **63**, 95-116.

Thurber C.H.; 1983: *Earthquake locations and three dimensional crustal structure in the Coyote Lake area, central California.* J. Geophys. Res., **88**, 8226-8236.

Virieux J. and Farra V.; 1991: *Ray tracing in 3D complex isotropic media: an analysis of the problem.* Geophysics, **56**, 579-594.

Waldhauser F., Kissling E., Ansorge J. and Mueller St.; 1998: *Three-dimensional interface modelling with two-dimensional seismic data: the Alpine crust-mantle boundary.* Geophys. J. Int., **135**, 264-278.

Corresponding author: D. Scafidi

Dipartimento per lo studio del Territorio e delle sue Risorse

Università di Genova

Viale Benedetto XV 5, 16132 Genova, Italy

phone: +39 010 3538098; fax +39 010 3538081; e-mail: scafidi@dipteris.unige.it